A Modified Hilbert-Huang Algorithm to Assess Spectral Parameters in Intense Exercise

Rebeca Goya-Esteban¹, Óscar Barquero-Pérez¹, Elena Sarabia-Cachadiña², José Naranjo-Orellana², José Luis Rojo-Álvarez¹

Rey Juan Carlos University, Fuenlabrada, Spain
Pablo de Olavide University, Sevilla, Spain

Abstract

Spectral indices are widely used to assess Heart Rate Variability (HRV) during exercise. HRV signal spectrum comprises two main bands, High Frequency (HF) and Low Frequency (LF), the first related to parasympathetic activity and the second related to both parasympathetic and sympathetic activity. HF and LF powers are mostly obtained by Fast Fourier Transform (FFT) based algorithms, however there is a major problem due to the non-stationary and non-linear properties of the signal. Also, FFT based algorithms usually provide single LF and HF indices for temporal windows of several minutes. In the present study, our aim was to achieve a deeper understanding on the autonomic regulation mechanisms during intense exercise and recovery. For this purpose, we obtained the instantaneous LF and HF indices using a modified version of the Hilbert-Huang (HH) algorithm to track the HRV evolution on eight male amateur triathletes in an All Out Exercise Test (AOET). Both HH-based and FFT-based algorithms revealed severely depressed LF and HF powers during exercise. However, using the FFT the LF/HF ratio was always lower than one during intense exercise, while the mean of the instantaneous LF/HF ratio was lower than one only in one case. The HH-based algorithm allowed a deeper insight about the sympathetic and parasympathetic balance during exercise.

1. Introduction

The cardiovascular system is mostly controlled by autonomic regulation through the activity of sympathetic and parasympathetic pathways of the Autonomic Nervous System (ANS). Analysis of Heart Rate Variability (HRV) allows insight in this control mechanisms [1]. A wide number of HRV indices have been proposed in the literature, among them spectral indices are widely used to assess HRV during exercise. HRV signal spectrum comprises two main spectral bands, High Frequency (HF), in 0.15-0.4

Hz, and Low Frequency (LF), in 0.04 - 0.15 Hz, the first related to parasympathetic activity and the second related to both parasympathetic and sympathetic activity [2]. During exercise it is generally assumed that Heart Rate (HR) increases due to both a parasympathetic withdraw and an augmented sympathetic activity. However, some authors disagree with the former statement, and also, there is a major problem when computing the LF and HF indices due to the non-stationary, and non-linear properties of the signals [1]. HF and LF powers are mostly obtained by Fast Fourier Transform (FFT) based algorithms. However, for this approach, the data must be strictly periodic or stationary, otherwise, spurious harmonic components can be induced and the consequence is a misleading energyfrequency distribution [3]. Further, FFT based algorithms usually provide LF and HF indices for temporal windows of several minutes, due to the requirements on spectral resolution. However, a single value of the indices will not be able to capture changing dynamics on the system within these windows. Time-frequency techniques constitute a major improvement respect to the described limitations.

In this work, we used an adapted version of the Hilbert-Huang (HH) algorithm to obtain the instantaneous LF and HF indices. This allowed to track the LF and HF indices before, during and after an All Out Exercise Test (AOET), rather than obtaining a single index value for each stage. The aim was to achieve a deeper understanding on the autonomic regulation mechanisms during intense exercise and recovery.

The structure of the paper is as follows. First, the dataset and data preprocessing is presented. Next, the methods and the data analysis are described, and the results are presented. Finally, conclusions are summarized.

2. Dataset

The dataset for this study consisted of HR recordings from eight male amateur triathletes. Information on the inclusion criteria and recording conditions can be found in [4]. All recordings were obtained while subjects were sitting on a cycle ergometer. The protocol included 5 minutes of HR recording in resting conditions before exercising. Afterwards, subjects started an incremental exercise test which comprised 4 consecutive phases of 4 minutes. In the first three phases, subjects cycled at 50 rpm with 1, 2, and 3 Kp of load. The last part of the test was the so-called 'All Out', in which subjects cycled as fast as they could with 5 Kp of load during 4 minutes for achieving maximal exercise capacity. HR was recorded in the 'All Out' step. The exercise test was followed by 5 minutes of recovery (subjects remained seated on the cycle ergometer without cycling) in which HR was also recorded.

RR intervals were collected using a Firstbeat Bodyguard (Firstbeat Technologies Oy^{TM} , Finland) heart monitor, with sampling frequency of 1000 Hz. The recordings were preprocessed to exclude artifacts by eliminating RR intervals lower than 200 ms and greater than 2000 ms, as well as those which differed more than 20% from the previous and the subsequent RR intervals [5]. Removed RR intervals were replaced by conventional spline interpolation.

3. Methods

The HH algorithm is a time-frequency technique consisting of two parts. First, the Empirical Mode Decomposition (EMD) procedure decomposes the signal into Intrinsic Mode Functions (IMF), putting forward the scale characteristics embedded in the signal. Second, the Hilbert Transform (HT) is applied to the IMFs, yielding a time-frequency representation, the Hilbert Spectrum [3, 6].

An IMF satisfies two conditions: (1) the number of extrema and the number of zero crossings must be either equal or differ at most by one; and (2) at any point, the mean value of the envelope defined by the local maxima and the envelope defined by the local minima is zero. In order to obtain a meaningful instantaneous frequency, an arbitrary signal must be reduced into IMF components. Consequently, for real signals, we can have more than one instantaneous frequency at a time. The EMD method reduces the signal into the needed IMFs. Given a signal x(t), the procedure starts identifying all the local maxima and minima. All the local maxima are then connected by a cubic spline curve as the upper envelope $e_u(t)$. Similarly, all the local minima are connected by a spline curve as the lower envelope $e_l(t)$. The mean of the two envelopes is denoted as $m_1(t) = (e_u(t) + e_l(t))/2$, and it is subtracted from $\mathbf{x}(t)$ to obtain the first component $h_1(t) = x(t) - m_1(t)$. The above procedure is referred as the sifting process. Since $h_1(t)$ still contains multiple extrema between zero crossings, the sifting process is performed again on $h_1(t)$. This process is applied repetitively to the component $h_k(t)$ until the first IMF $c_1(t)$, which contains the shortest period component of the signal, is obtained. We can separate $c_1(t)$ from the data by $r_1(t) = x(t) - c_1(t)$. Since the residue,

 $r_1(t)$ still contains contains information of longer period components, it is treated as new data and subjected to the same sifting process. This procedure can be repeated on all the subsequent residues, and the result is

$$r_2(t) = r_1(t) - c_2(t), \dots, r_L(t) = r_{L-1}(t) - c_L(t)$$
 (1)

The whole procedure ends when the residue $r_L(t)$ is either constant, or a monotonic slope, or a function with only one extremum. The EMD produces L IMFs and a residue signal. In this work we used the EMD implementation described in [7].

Having obtained the IMFs, we can apply the HT to each IMF, and compute the instantaneous frequency. The HT of a real signal x(t) is defined as

$$y(t) = \frac{1}{\pi} P \int_{-\infty}^{\infty} \frac{x(\tau)}{t - \tau} d\tau \tag{2}$$

where P indicates the Cauchy principal value. With this definition, $\mathbf{x}(t)$ and $\mathbf{y}(t)$ form the complex conjugate pair, so we can have an analytic signal, $z(t) = x(t) + iy(t) = a(t)e^{i\theta_t}$, in which

$$a(t) = \sqrt{x^2(t) + y^2(t)}, \quad \theta(t) = \arctan\left(\frac{y(t)}{x(t)}\right) \quad (3)$$

The instantaneous frequency is defined using the instantaneous phase variation,

$$\omega = \frac{d\theta(t)}{dt} \tag{4}$$

After performing the HT in each IMF component, we can express the signal in the form

$$x(t) = \sum_{j=1}^{L} a_j(t) \exp\left(i \int \omega_j(t) dt\right)$$
 (5)

which enables to represent the amplitude and the instantaneous frequency as functions of time. This time-frequency distribution is designated as the Hilbert spectrum, $H(\omega,t)$, which represents the cumulated amplitude over the entire data span in a probabilistic sense. The squared values of amplitude can be substituted to produce the Hilbert energy spectrum as well. It In this work we obtained the Hilbert spectrum with the implementation available in [8]. It is possible to achieve a measure of the energy of the signal with respect to time, computing the instantaneous energy densitity level, IE, as

$$IE(t) = \int_{\omega} H(\omega, t)^2 dw \tag{6}$$

In this work the last IMF was eliminated to detrend the signal. Next, two band pass filters, with pass bands matching the LF and HF bands (ω_{LF} and ω_{HF}), were used to

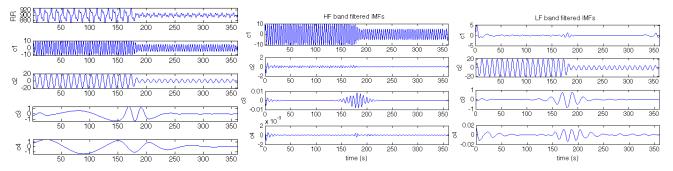


Figure 1. HRV synthetic signal (RR) and the corresponding IMFs obtained by EMD decomposition (left panel). HF band (middle panel) and LF band (right panel) filtered IMFs.

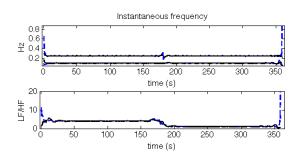


Figure 2. Instantaneous frequency computed with the original (dashed) and filtered (continuous) c1 and c2 (top). Instantaneous LF/HF ratio obtained with the original (dashed) and filtered (continuous) IMFs (bottom).

filter the remaining IMFs. Both filters were 6^{th} order infinite impulse response of Butterworth type and zero phase distortion. The instantaneous amplitudes and frequencies were obtained from the Hilbert spectrum. Finally, the instantaneous LF and HF powers were obtained by equation (6) selecting $\omega = \omega_{LF}$ and $\omega = \omega_{HF}$, respectively.

Mean LF and HF instantaneous indices were also obtained in each stage for comparison with those obtained for the same recordings with the Firstbeat Health Software, which uses an FFT-based algorithm .

4. Results

The method was first validated using a simulated HRV signal composed by the sum of two sinusoidal functions, with frequencies corresponding to simplified LF and HF contributions, and an offset corresponding to the mean value of the HRV signal, i.e.,

$$RR = A_0 + A_{LF}sin(\omega_{LF}t) + A_{HF}sin(\omega_{HF}t)$$
 (7)

where $A_0 = 900$, $\omega_{LF} = 0.1 \cdot 2\pi$, $\omega_{HF} = 0.25 \cdot 2\pi$, A_{LF} and A_{HF} were 20 and 10 respectively for the first 3 minutes of the signal, and both 5 for the last 3 minutes.

Figure 1 (left panel) shows the synthetic HRV signal (RR) and its EMD decomposition until c4. The amplitudes of c1 and c2 are related to the amplitudes of the two sinusoidal components of RR oscillating at 0.25 and 0.1 Hz, respectively. The rest IMFs, c3-c4, show very low amplitudes. It also shows the HF band (middle panel) and LF band (right panel) filtered IMFs. In the middle panel, c1 contains the information related to the HF sinusoidal component while the rest IMFs have amplitudes close to zero. In the right panel, c2 contains the information related to the LF sinusoidal component while the rest IMFs have amplitudes close to zero.

Figure 2 (top) shows the computed instantaneous frequency of the original c1 ($m \pm std$: 0.2513 \pm 0.0224) and c2 (0.0997 \pm 0.0062), and the instantaneous frequency of the HF band (c1) (0.2501 ± 0.0038) and LF band (c2) (0.1000 ± 0.0045) filtered ones. With the nonfiltered IMFs abrupt instantaneous frequency values were obtained for the signal endings (mainly for c1). In real signals, different IMFs can contain frequencies in the LF and HF bands, therefore, to obtain the LF and HF indices, all the IMFs are taken into account. Figure 2 (bottom) shows the instantaneous LF/HF ratio computed with the original IMFs, (4.0359 ± 0.5676) for the three first minutes, 1.1091 ± 1.0302 for the three last minutes), and the instantaneous LF/HF ratio computed with the filtered IMFs $(3.9758 \pm 0.3914$ for the three first minutes, $1.1271 \pm$ 0.4295 for the three last minutes). Theoretical values are 4 and 1, for the first and the last part of the synthetic HRV signal respectively. With the nonfiltered IMFs, we obtained higher std values due to abrupt discontinuities at signal endings. Moreover, smoother instantaneous values were obtained through the whole signal with the filtered IMFs.

LF, HF and LF/HF instantaneous indices were computed for the triathletes in the different protocol stages, the 5 minutes in resting conditions, the *All Out* phase of the exercise test, and the five minutes of the recovery stage. Figure 3 depicts the time evolution of the population mean

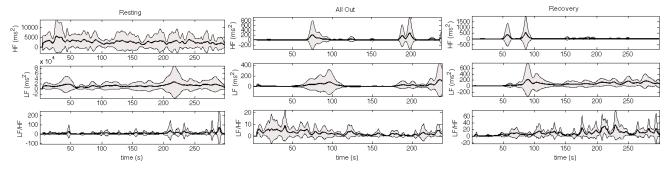


Figure 3. Instantaneous LF, HF and LF/HF indices, population mean and standard deviation (shaded bands): resting stage (left), *All Out* phase (middle), and recovery stage (right).

and standard deviation (shaded bands). It shows a high variability on the indices within each stage. In the resting stage this variability is smoother in percentage units, while the *All out* phase presents more abrupt variations. The beginning of the recovery stage also presents abrupt variations, and then the system returns to smoother variations. It can be seen that the indices were extremely depressed during the *All out* phase compared to the resting stage and that the ratio LF/HF was lower in this stage.

Considering the mean values of the instantaneous indices for each stage and the indices values obtained by the FFT-based algorithm, in the resting stage the LF index was higher than the HF index (for 7 out of 8 athletes) with both algorithms. During the *All out* phase the LF index was lower than the HF index with both algorithms, however the LF/HF ratio was always lower than one with FFT-based algorithm, while the mean of the instantaneous LF/HF ratio was always higher than one except for one case. In the first part of the recovery stage, HF index was still higher than the LF index, but then the relation was reversed, although the indices values continued very depressed in this stage compared to the resting values.

5. Conclusions

The modification on the HH algorithm introduced in this work provided smoother variation of the instantaneous frequency and spectral indices, and improved the estimation of these signals endings. With this algorithm, we tracked the spectral indices during an AOET, which allowed a deeper insight on the autonomic regulation mechanisms than usually used FFT-based algorithms, which may be inaccurate and lost information due to temporal averaging.

Acknowledgements

This work has been partially supported by Research Project TEC2010-19263 and OBP is supported by FPU grant AP2009-1726 (both from Spanish Government).

References

- [1] Aubert AE, Seps B, Beckers F. Heart rate variability in athletes. Sports Medicine 2003;33(12):889–919.
- [2] Camm A, Malik M, Bigger J, et al. Heart rate variability: standards of measurement, physiological interpretation, and clinical use. Task Force of the European Society of Cardiology and the North American Society of Pacing and Electrophysiology. Circulation 1996;93(5):1043–1065.
- [3] Huang NE, Shen Z, Long SR, et al. The empirical mode decomposition and the hilbert spectrum for nonlinear and nonstationary time series analysis. Proceedings of the Royal Society of London Series A Mathematical Physical and Engineering Sciences 1998;454(1971):903–995.
- [4] Goya-Esteban R, Barquero-Pérez O, Sarabia-Cachadina E, et al. Heart rate variability non linear dynamics in intense exercise. In Computing in Cardiology, 2012. IEEE, 2012; 177–180.
- [5] Malik M, Cripps T, Farrell T, Camm A. Prognostic value of heart rate variability after myocardial infarction. A comparison of different data-processing methods. Medical and Biological Engineering and Computing 1989;27(6):603–11.
- [6] Fonseca-Pinto R. A New Tool for Nonstationary and Nonlinear Signals: The Hilbert-Huang Transform in Biomedical Applications, Trends in Electronics, Communications and Software. InTech, 2011.
- [7] Rilling G, Flandrin P, Gonçalves P, et al. On empirical mode decomposition and its algorithms. In IEEE-EURASIP Workshop on Nonlinear Signal and Image Processing, volume 3. 2003; 8–11.
- [8] Rilling G. The time-frequency toolbox, 2007. URL http://tftb.nongnu.org/.

Address for correspondence:

Rebeca Goya-Esteban Signal Theory and Communications Department Rey Juan Carlos University. D202 Camino del Molino s/n 28943 Fuenlabrada, Madrid (Spain)

Phone: +34 91 488 84 49 rebeca.goyaesteban@urjc.es